An empirical geomorphology-based approach to the spatial prediction of soil thickness at catchment scale

An empirical geomorphology-based approach to the spatial prediction of soil thickness at catchment scale

Filippo Catani,[1] Samuele Segoni,[1] and Giacomo Falorni[1]

Received 15 September 2008; revised 15 October 2009; accepted 12 November 2009; published 5 May 2010.

[1] Catchment modeling in areas dominated by active geomorphologic processes, such as soil erosion and landsliding, is often hampered by the lack of reliable methods for the spatial estimation of soil depth. In a catchment, soil thickness *h* can vary as a function of many different and interplaying factors, such as underlying lithology, climate, gradient, hillslope curvature, upslope contributing area, and vegetation cover, making the distributed estimation of *h* challenging and often unreliable. In this work we present an alternative methodology which links soil thickness to gradient, horizontal and vertical slope curvature, and relative position within the hillslope profile. While the relationship with gradient and curvature should reflect the kinematic stability of the regolith cover, allowing greater soil thicknesses over planar and concave areas, the distance from the hill crest (or from the valley bottom) accounts for the position within the soil toposequence. This last parameter is fundamental; points having equal gradient and curvature can have significantly different soil thickness due to their dissimilar position along the hillslope profile. The proposed model has been implemented in a geographic information system environment and tested in the Terzona Creek basin in central Italy. Results are in good agreement with field data (mean absolute error is 11 cm with 8.5 cm standard deviation) and average errors are lower than those obtained with other topography-based methods, where mean absolute error ranges from 47 cm for a model based on curvature, position, and slope gradient to 94 cm for a model based solely on slope gradient. As a further test, the predicted soil thickness was used to determine derived quantities, such as the factor of safety for landsliding potential. Our model, when compared to other empirical methods, returns the best results and, therefore, can improve the prediction of soil losses and sediment production when utilized in conjunction with hydrological and landsliding models.

Citation: Catani, F., S. Segoni, and G. Falorni (2010), An empirical geomorphology-based approach to the spatial prediction of soil thickness at catchment scale, *Water Resour. Res.*, *46*, W05508, doi:10.1029/2008WR007450.

1. Introduction

[2] Soil thickness *h*, intended here as depth to bedrock (DTB), or depth to the first marked change in hydrologic properties, is widely recognized as a controlling factor in numerous surface and subsurface processes (e.g., landscape evolution [*Heimsath et al.*, 1997, 2000, 2001b], soil conservation [*Gabet and Dunne*, 2003], crop protection [*Schumacher et al.*, 1999], sediment budgets [*Reid and Dunne*, 1996], landsliding [*Johnson and Sitar*, 1990; *Wu and Sidle*, 1995; *Van Asch et al.*, 1999], and soil moisture storage and conservation capacity [*Boer et al.*, 1996; *Lexer and Honninger*, 1998]). This notwithstanding, it is still one of the least understood and difficult to measure physical variables of the hillslope system at catchment scale. Traditional soil mapping at the 1:25,000 to 1:100,000 scales usually does not include continuous information on spatially variable soil properties [*Boer et al.*, 1996] and direct measurement of *h* is only possible for small and well-monitored test sites. Satellite or airborne remote sensing techniques are ineffective, as to date they are only capable to resolve the first few centimeters of soil [*Liang*, 1997].

[3] These difficulties are amplified by the lack of reliable methods for the prediction of spatially distributed soil depth as few models are capable of describing the behavior of *h* as a random spatial function. At a more local scale, the evolution and development of soil horizons and layers through time are well understood. Early works on soil formation and classification date back to the beginning of the 20th century [e.g., *Milne*, 1935] while more recent contributions on the same subject are coded into the fundamentals of soil science [e.g., *Hillel*, 1980, 1998; *Jenny*, 1941, 1980; *United States Soil Conservation Service*, 1975].

[4] These contributions converge upon a couple of issues which are of direct interest for the prediction of DTB: the importance of the Late Quaternary evolution in setting the controlling conditions and the key role played at basin scale by the local differences in lithology and morphometry. The latter is intended here as a complex combination of hillslope shape and geometric factors. In particular, there is general agreement [*Gessler et al.*, 2000; *Ziadat*, 2005; *Goodman*,

[1]Department of Earth Sciences, University of Firenze, Florence, Italy.

0043-1397/10/2008WR007450

1999] regarding the relevance of the relative position within the soil catena, as well as slope gradient and elevation. This knowledge has not yet been distilled into a single expression combining DTB factors at basin scale and, for hydrological or slope stability purposes, soil depth is still usually estimated from very simple models. Commonly used approaches are based on a linear correlation between soil thickness and elevation or slope gradient [e.g., *Saulnier et al.*, 1997]. The performance of such models is usually poor due to the lack of consideration of fundamental parameters such as slope curvature, lithology and relative position within the soil sequence or catena.

[5] Better results, although usually site specific, were described by *Boer et al.* [1996] and *Tsai et al.* [2001] using multivariate statistical models that correlate soil depth with a combination of independent variables assumed to influence DTB spatial distribution. Over limited areas, *Moore et al.* [1993] and *Odeha et al.* [1994] found that the thickness of the A horizon correlated well with topographic attributes such as slope angle and the wetness index (as defined by *Beven and Kirkby* [1979]).

[6] Other studies [*Heimsath et al.*, 1999, 2000, 2001a, 2001b; *Mudd and Furbish*, 2004, 2006; *Saco et al.*, 2006] concentrate on the understanding and modeling of the temporal evolution of soil thickness over geological time scales. These studies have their roots in the early works of *Gilbert* [1877], *Jenny* [1941], *Hack* [1960], *Carson and Kirkby* [1972], and others that hypothesized the dependence of soil properties on topography and suggested the use of a mass conservation equation for soil transfer. Using a similar approach *Park et al.* [2001] highlighted a clear relationship between soil depth and the terrain characterization index, a morphometric measure of soil transport capacity. At the same time, they showed significant statistical correlations between h and a number of terrain attributes such as surface curvature, topographic wetness index and upslope contributing area. Deterministic methods based on these factors have been used by many authors in models of soil depth evolution [*Heimsath et al.*, 1997, 1999, 2000, 2001a, 2001b; *Martin*, 2000; *Braun et al.*, 2001; *Mudd and Furbish*, 2004, 2006; *Saco et al.*, 2006]. These are usually based on expressions for soil production and transport (whose rates are assessed by cosmogenic nuclides measurements performed at discrete points) that solve the conservation of mass equation. Assuming steady state erosion and the predominance of slope-dependent erosion processes such as soil creep, they predict soil depth as a function of hillslope curvature at the slope scale or over small test areas [*Heimsath et al.*, 1997, 1999, 2001a, 2001b; *Braun et al.*, 2001; *Saco et al.*, 2006]. In high-order catchments, cosmogenic nuclides measurements at discrete points become too expensive and samples are often collected at basin outflow points. Soil production rate is then extrapolated to the subtended basin [*Bierman and Steig*, 1996]. In large areas with heterogeneous lithology these averaged data may lead to incorrect estimations of local soil depth [*Heimsath et al.*, 2001b]. Thus, despite being useful for landscape evolution models, such methods are less suitable at present for instantaneous soil thickness predictions at broad scales for applied purposes. Moreover, while the hypothesis of landscape equilibrium (steady state) with absence of mass movements (such as landslides) produces good results in the upper convex portions of the hillslopes, outcomes are poorer on concave midslopes and footslopes, especially in tectonically young regions where mass movements have a significant influence on soil thickness distribution [*Densmore et al.*, 1997, 1998; *Heimsath et al.*, 1999, 2001b; *Roering et al.*, 1999].

[7] These drawbacks can be avoided if, instead of predicting soil depth evolution, we attempt to predict the instantaneous values of h over a discrete space at a chosen spatial resolution. In such cases a simple empirical model valid over the entire catchment can be derived from a set of empirical relationships linking the parameters of the deterministic formulation to the soil depth measured in the field for both concave and convex areas. In the following pages we develop a model of this type, based on topographic Digital Terrain Model (DTM) data, digital geological maps and general information on the land-surface units. Ideally, the model should be able to predict the depth of the colluvial and residual layers with an accuracy compatible with the requirements of slope stability and rainfall-runoff models. We have calibrated and validated the model in a study catchment located in central Italy, the Terzona basin. The main characteristics of the model are as follows: (1) catchment-scale analysis, (2) possible implementation within a geographic information system (GIS) environment, (3) wide availability and low cost of the required parameters, and (4) more balanced consideration of topographic attributes in conjunction with geological and geomorphological factors.

2. Test Site Description

[8] The test site for the calibration and validation of the model was the Terzona Creek Basin (24 km^2) which is located in central Italy, about 20 km south of Florence (Tuscany). The Terzona is a mountain stream with a marked erosive behavior which flows in a hilly region without developing a proper floodplain. Geologically, the area (Figure 1) is characterized by the prevalence of Pliocene to Quaternary granular deposits outcropping in the central and northern parts of the catchment. These represent post-orogenic deposits of extensional intermontane basins that are common to the whole Northern Apennine [*Martini and Vai*, 2001]. Subhorizontal layers of pliocenic conglomerates, deeply incised by the Terzona Creek, are the dominant lithology in the basin. Ridge tops in this area are often occupied by "Pianalto," a Quaternary terrain made up of fine, silty sediment that includes Pleistocene paleosols. This geological domain gives rise to a smooth landscape that is strongly influenced by agriculture. On the hillslopes small woods are surrounded by vineyards and olive groves. Buildings, mainly isolated farmhouses or country houses, are concentrated on the main ridges. In the southeastern portion of the catchment the geology changes significantly, giving way to the Early Tertiary fold and thrust belt units of the Northern Apennines composed of marly and calcareous flysch, belonging to the Sillano and Monte Morello formations. These terrains possess a greater average mechanical strength than the transgressive marine and lacustrine deposits filling the intermontane basin and produce a higher-relief landscape, with elevations that reach 512 m above sea level. Small forests are common in this area. To the south, a third geological domain is represented by the shaley clays of the

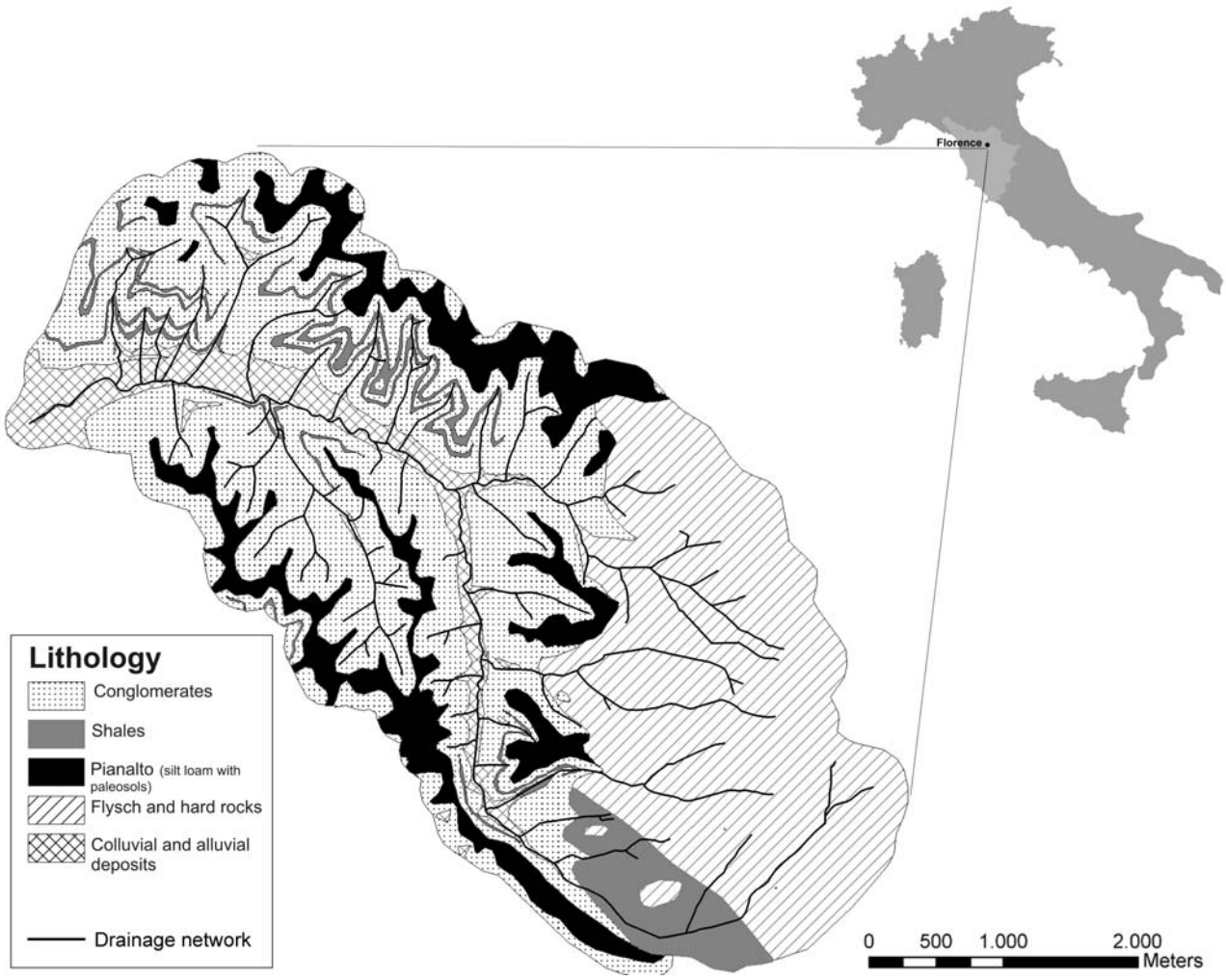

Figure 1. Main lithological units of the Terzona basin. See Table 2 for more details.

Tuscan Series. Here, again, relief is gentle and vegetation sparse. Soil formation and development varies within each of these three geological domains, as will be clarified in section 3. From a geomorphological standpoint the area is characterized by the presence of several landslides, mainly located within the conglomerates of the first geological domain and whose activity is characterized by an alternating of periods of stasis and sporadic episodes of movement. Rates of movement are generally very low (10^{-4} to 10^{-2} m d^{-1}) but the sediment quantities involved are quite large (10^4 to 10^6 m^3), thus making landsliding an important landscape shaping process in the area [*Catani et al.*, 2005 and references therein]. On the other hand, newly formed slope failures are relatively rare and are usually represented by small slumps or falls along channel banks, road cuts or erosion scarps.

3. Methodology

[9] Under the assumption that we are interested in the prediction of the present instantaneous local values of depth to bedrock (DTB) at every point in a catchment, we can modify the basic equations of conservation of mass for the soil column proposed by *Heimsath et al.* [1997, 1999] and *Minasny and McBratney* [1999, 2001] in which the continuity equation is expressed as

$$\rho_s \frac{\partial h}{\partial t} = -\rho_r \frac{\partial b}{\partial t} - \rho_s \frac{\partial w}{\partial t} - \nabla \cdot (\rho_s \mathbf{q_s}), \tag{1}$$

where ρ_s and ρ_r are soil and rock density, $\mathbf{q_s}$ is the soil flux, h is surface layer thickness, b and w are the elevation of bedrock and ground surface with respect to an arbitrary elevation reference, $\partial b/\partial t$ is the rate of soil production from bedrock and $\partial w/\partial t$ is the soil lowering rate due to chemical weathering.

[10] First, the rate of soil production from bedrock $\partial b/\partial t$ and that of soil chemical dissolution $\partial w/\partial t$ can be replaced with implicit constant coefficients within boundary conditions that depend locally on lithology and geological history.

[11] Second, for simple creep [*Dietrich et al.*, 1995], depth-dependent creep [*Braun et al.*, 2001] and overland flow erosion [*Moore and Burch*, 1986], it can be shown that soil transfer by diffusion depends mainly on slope. In fact, in the right hand side of equation (1), which expresses soil loss for sediment transport, the sediment flux can be expressed as

$$q_d = -K_d \nabla z \tag{2}$$

for soil creep [*Dietrich et al.*, 1995]

$$q_v = -K_v h_c^m (\nabla z)^n \tag{3}$$

for depth-dependent creep [*Braun et al.*, 2001]

$$q_w = -K_w A^k (\nabla z)^p \tag{4}$$

for overland flow [*Moore and Burch*, 1986], where K_d, K_v, and K_w are the relative diffusion or advection coefficients, h_c is soil creep depth, A is upslope contributing area, z is elevation, m, n, k and p are empirically defined constants.

[12] Substituting (2), into (1) gives a relationship in the form

$$\nabla \rho_s q_s \propto -K\left(\nabla^2 z\right) \tag{5}$$

that links soil losses to hillslope laplacian curvature. This hypothesis is supported by several experiments and field observations [*Heimsath et al.*, 1999, 2001a; *Braun et al.*, 2001; *Park et al.*, 2001], which show that local soil depth is inversely correlated with slope curvature. However, curvature is only one part of the problem since equation (5) ignores the contribution of active processes that depend on slope length or on upslope contributing area. Their impact on soil thickness distribution will be taken into account by linking them to position along the hillslope profile, which will be discussed further in the following paragraphs.

[13] Third, the net contribution of soil losses and gains due to mass movements can be linked to threshold processes triggered by slope gradient that in some cases decouple relief from soil losses [*Roering et al.*, 2001; *Montgomery and Brandon*, 2002]. The authors show that when a threshold slope is approached, landslides of increasing size and frequency are triggered, influencing the hillslope or catchment DTB distribution and progressively reducing curvature with increasing slope gradient.

[14] However, it is also well known that local hillslope geometry is not the only factor controlling regolith thickness: two different points along a hillslope profile can have the same slope gradient and curvature but still have different soil characteristics, due to their different relative position [see, e.g., *Arnett and Conacher*, 1973; *Conacher and Dalrymple*, 1977; *Armstrong*, 1987; *Moore et al.*, 1993; *Gessler et al.*, 1995]. The effect of hillslope processes, history, geology and of environmental settings are remarkably important in controlling the distribution of soil parameters [*Milne*, 1935; *Jenny*, 1941; *Hillel*, 1980; *McFadden and Knuepfer*, 1990; *Selby*, 1993; *Schlunegger et al.*, 2002; *Saco et al.*, 2006]. Furthermore, soil thickness evolution models do not explicitly take into account the presence of active landslides [*Roering et al.*, 2001] that can decouple hillslope curvature from regolith thickness at the footslopes where profile convexity is generated by landslide bodies. In such cases, profile convexity is actually an indication of higher DTB, as it is related to large soil masses [*Rapisarda*, 2007], while the convexities characterizing hilltops are usually related to erosional morphologies and to shallower soil depths. We propose here a method that encompasses such traditionally neglected cases by spatially partitioning the study area into two-dimensional land-surface units (TLU) which are based on similar relationships between topography, active geomorphic processes and soil thickness. TLUs are delineated from digital geological and geomorphological maps, field surveys and DTM data. A similar approach is suggested by *Brundsen et al.* [1975], *Moore et al.* [1993], and *Selby* [1993] to assess the impact and relevance of different surface processes on various hillslopes.

[15] Once the TLUs have been defined, it is then necessary to explicitly consider the position of a point along the hillslope profile and to express it as a function of the regolith catenary sequence. This requires the following two steps: (1) the calculation of the actual relative position p of a point along the hillslope and (2) the translation of p into an index of relative thickness η based on the known local toposequence pertaining to a given TLU.

[16] In a raster DTM, p can be determined by a simple recursive algorithm that calculates the shortest upslope hydrologic distance to the hilltop and the shortest downslope path to the channel network, following the method proposed by *Tucker et al.* [2001].

[17] This number, which ranges from 0 at the crest to 1 at the channel, is then translated into a DTB value by combining p with the particular catenary sequence of the TLU. To estimate soil thickness with this model it is not necessary to perform a complete analysis and classification of the soil toposequences present within an area. A simpler approach that identifies large land-surface units according to the "nine-unit" model of *Conacher and Dalrymple* [1977] through detailed field surveys is adequate. The nine-unit land-surface model defines the three-dimensional space of a hillslope as a set of adjacent units differentiated on the basis of the dominant processes acting on them. It extends from hilltops (or drainage divides) to channels and from the lowermost weathered material (C horizon) within the soil to the ground surface [*Conacher and Dalrymple*, 1977; *Selby*, 1993] thereby linking soil-related forms and slope processes. This approach, although subjective and simplistic, makes it possible to partition the basin into TLU classes on the basis of the average land-surface characteristics. The DTB model will then be parameterized differently for each TLU.

[18] In the case of the Terzona catchment, the following three main types of hillslope morphologies were identified (Figure 2):

[19] 1. Convex profiles, typical of relatively young hillslopes dominated by creep-like diffusive processes in which all the material eroded from the slope reaches the footslope and is then removed by streams. In this case soil thickness is inversely proportional to curvature, as creep erosion rates increase with increasing convexity.

[20] 2. Convex to concave profiles, the classical mature hillslope [*Armstrong*, 1987] where upslope erosive processes (mainly wash and creep) produce convex shapes while the eroded material partially accumulates downslope in gentle concave areas. As in the previous case, DTB and curvature are inversely correlated: in the upper portion of the hillslope erosion increases with convexity, leading to thinner soils, and field observations [*Segoni*, 2008] confirm that in the concave lower sections soil depths are higher; in both sections of the slope the inverse correlation still holds.

[21] 3. Convex to concave to convex profiles, typical of many of the Northern Apennine's landslide areas, are similar to the previous case with the exception of the presence of a convex footslope unit occupied by the deposits of deep-seated mass movements. As opposed to the other regimes,

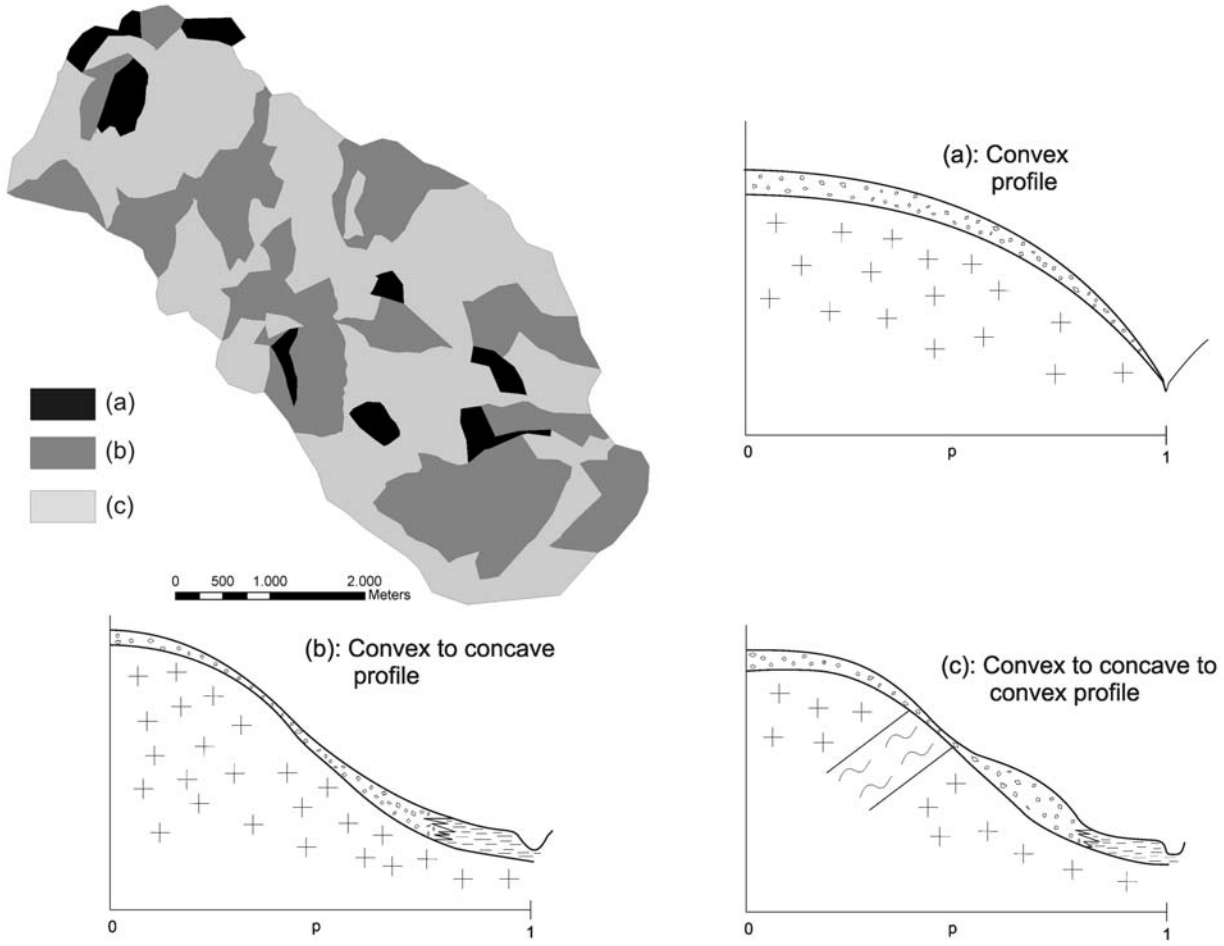

Figure 2. Schematic representation and spatial distribution of the three types of hillslope morphologies encountered within the Terzona catchment. Every slope draining into a first- or higher-order stream has been classified through field surveys and DTM analyses. The relationship between soil depth and profile curvature is parameterized differently for each typology.

this colluvial area is characterized by a direct correlation between curvature and depth to bedrock.

[22] For each of these profiles the curvature is translated into a nondimensional index C, whose value ranges between 0 and 1, by means of linear normalization. This index expresses the expected DTB of each pixel with respect to slope curvature.

[23] In addition, TLU type links the p factor and the relative DTB value by means of the catenary position within the hillslope profile, represented by the adimensional scale factor η (where $0 \leq \eta \leq 1$).

[24] The following three TLUs identified in the Terzona catchment are related to the lithology of the bedrock (Figure 1).

[25] 1. For flysch and hard rocks (Figure 1), in the Terzona basin the areas with massive or layered rocks have a typical hillslope toposequence composed of an interfluve where shallow soil depths suggest that erosion rates are high relative to rates of soil production. The eroded material moves downslope and partially accumulates on the midslope, where it is transported to the base of the slope by intermittent mass movements. The largest DTB values are observed in the colluvial deposits at the footslope close to the channels. The latter have a marked erosive behavior and do not develop an alluvial plain. In this TLU the p–η relationship is derived on the basis of qualitative observations and direct measurements performed over a subset of calibration points by assuming that η increases linearly from the minimum value ($\eta = 0$) in the interfluves (p = 0) to the maximum ($\eta = 1$) in the toeslope (p = 1). η is therefore set equal to p [*Segoni*, 2008].

[26] 2. For conglomerates ("Conglomerates," "Pianalto" and "Colluvial and alluvial deposits" lithologies in Figure 1), in the areas where the bedrock is made up of mostly granular material the divide is occupied by the Pianalto silty loam, which gives rise to flat morphologies with considerably thick soils. The shallowest soils are usually found on the convex creep slope, while the largest DTB values are found in the alluvial plain. Consequently, η has relatively high values (η around 0.6) at p = 0, decreases to the minimum in correspondence of p = 0.4 and then rapidly increases again to the maximum value ($\eta = 1$) at p = 1 (corresponding to the alluvial plain, mainly constituted by colluvial material from the surrounding hillslopes and by sediments carried from upstream without lateral erosion and redeposition) [*Segoni*, 2008; *Benvenuti et al.*, 2007]. The corresponding p–η trend can be approximated by a polynomial function of the form $\eta = a\,p^4 + b\,p^3 + c\,p^2 + d\,p + e$, where the coefficients from a to e are estimated from the η value expected for dis-

Table 1. Geotechnical Parameters of the Formations Present in the Study Area[a]

Geological Formation or Unit	Abbreviation	Prevalent Lithology	Threshold Slope Angle	c (KPa)	k_s (m/s × 10^{-6})	φ
Sillano formation	Sil	Clayey shales	35°	6.5	7.53	22°
Monte Morello formation	Mll	Limestones and marly limestones (subordinately marly shales)	35°	3.0	7.53	30°
San Polo marls	Poo	Silty marls and marls, with interbedding of silts and fine-grained sandstones	27°	6.5	0.33	22°
Ponte a Elsa syntheme, silt-clay lithofacies	Ela	Silts and clays	27°	4.0	6.56	22°
Fiume Elsa syntheme	E2	Weathered conglomerates (sub. sandy silts)	45°	3.0	6.56	25°
San Casciano syntheme: pebbles lithofacies	Cc	Conglomerates	45°	1.5	2.06	30°
San Miniato syntheme: pebbles lithofacies	Mc	Conglomerates	45°	1.5	2.06	30°
Ponte a Elsa syntheme	Eca	Conglomerates	45°	1.5	2.06	30°
San Casciano syntheme: sand-silt lithofacies	Cl	Sands and silts	30°	3.0	0.33	25°
San Miniato syntheme: sand-silt lithofacies	Mla	Sands and silts	30°	1.5	0.33	30°
Fiume Elsa syntheme	E1	Sandy silts (weathered conglomerates)	30°	3.0	4.98	25°
Slope debris	a3		30°	1.5	6.56	30°
Colluvial and eluvial deposits	a4		30°	1.5	6.56	30°
Alluvial fans	Alf		30°	1.5	6.56	25°
Recent alluvial deposits	b		30°	0	6.56	30°

[a]The threshold slope angle is used in the GIST model, while c, k_s (saturated hydraulic conductivity), and φ are used in the slope stability equation.

crete p values on the basis of qualitative observations and direct measurements performed over a subset of calibration points.

[27] 3. In the case of cohesive soils ("Shales" lithology in Figure 1), the bedrock is mainly composed of compact clays and tectonized shales that give rise to smooth slopes with a typical toposequence that is similar to that of the previous TLU except for the absence of small cliffs and less developed interfluves. As can be expected, η exhibits a similar trend to the previous case, notwithstanding its lower value in the interfluve (p = 0). It then decreases rapidly to reach the minimum value (η almost zero) at p around 0.2 before rising again to reach the maximum in the alluvial plain (p = 1) [*Segoni*, 2008; *Benvenuti et al.*, 2007]. The polynomial function $\eta = a\,p^4 + b\,p^3 + c\,p^2 + d\,p + e$ is again appropriate for describing the identified trend and the coefficients are determined as in the previous case.

[28] The empirical relationships between p and η for each TLU class described above are based on field observations and calibrated on direct soil depth measurements (auxiliary material).[1]

[29] In a final step, sediment loss by intermittent landsliding in the upper portions of the hillslopes is taken into account by defining appropriate, lithology-dependent thresholds for the triggering of mass transport. This follows the approach of *Roering et al.* [2001], who found an exponential relationship between slope gradient and sediment flux with a sharp, rapid increase of the latter when a gradient threshold is approached. In our case, threshold values θ_{th} (intermediate between internal friction angle and Roering theoretical threshold) were selected for each different lithology according to the average mechanical characteristics of the terrain (Table 1). Threshold selection involved several steps. Since the regolith cover of the area is composed mainly of granular soils, a first estimate of the threshold angles is based on the internal friction angle typical of each lithology [see, e.g., *Bianchi et al.*, 2001; *Focardi and Garzonio*, 1983; *Canuti et al.*, 1982]. Subsequently, the values were modified to include the additional effect of cohesion and vegetation cover (apparent cohesion), based on a large statistical and back analysis study of more than 27000 historical landslides in the Arno River basin [*Catani et al.*, 2005]. Finally, the accuracy of the thresholds was verified on the basis of detailed analyses of hillslope profiles by observing, for each geological formation, the local slope angle most frequently associated to mass movements in the area.

[30] The final expression has the form

$$h = -K_c \cdot C \cdot \eta \cdot \psi^{-1}, \tag{6}$$

where h is soil thickness, K_c is a calibration parameter, C is the curvature-based index, η is the relative thickness linked to the catenary position, and ψ is the threshold-dependent contribution of landsliding. This last parameter is equal to $(1 + \tan\theta_{th})$ in the pixels with a local slope higher than the threshold angle and to 1 everywhere else. ψ accounts only for the detachment (loss of soil) in the upper slopes, while downslope accumulation is already explained by curvature. The three indexes discussed above (C, η and ψ^{-1}) express (in the form of pure numbers ranging from 0 to 1) the propensity of a point to accumulate soil cover, while the constant K_c, which is calculated for each lithology from the in situ measurements (Table 2), calibrates the formula and transforms the pure number to a metric value. We refer to this model as the Geomorphologically Indexed Soil Thickness (GIST) model.

4. Model Calibration and Validation

[31] The calibration of K_c is fundamental as it summarizes the effects of the TLU and catenary position for every cell. All morphometric computations were carried out in a raster-based GIS environment in which the base DTM had a horizontal resolution of 10 × 10 m and a vertical accuracy of about 0.5 m. The DTM was generated from stereo pairs of low-altitude aerial photographs integrated with point data from GPS field surveys. The TLU and the catenary sequence definition were determined from a survey based reclassification of detailed 1:5,000 scale geological and geomorphological maps [*Segoni*, 2008]. The geological formations were

[1]Auxiliary materials are available in the HTML. doi:10.1029/2008WR007450.

Table 2. Measured Soil Depth Parameters for the Main Lithologies[a]

Lithology	Geological Formation or Lithostratigraphic Unit	Minimum Measured Depth (cm)	Maximum Measured Depth (cm)
Flysch and hard rocks	Mll, Sil	0	40
Shales	Poo, Mla, Cl	0	43
Conglomerates	Cc, Mc, Eca	5	60
"Pianalto" paleosol	E1	21	65
Colluvial and alluvial deposits	Ela, E2, b, a3, a4, Alf	30	150

[a]For an explanation of the abbreviations see Table 1. These values are used for model calibration.

grouped into five units, mainly according to bedrock lithology: flysch and hard rocks, shales, conglomerates, Pianalto (silt loam terrains with paleosols) and a comprehensive unit including colluvial and alluvial deposits (Figure 1 and Tables 1 and 2).

[32] During fieldwork, carried out in the spring and summer of 2004, 217 direct measurements of soil depth were made from preexisting or newly excavated soil profiles (see two examples in Figure 3). These measures were divided in two subsets: the first was used to calibrate the various indexes and factors constituting the model, the second was used to perform a validation. The presence of woods, villages and large private properties prevented soil depth sampling over a regular network and explains why some clustering occurs. In any case, a representative number of measures, sufficient to correctly calibrate and validate the model, was obtained for every lithology, catenary unit and TLU. Measured depths for each lithological class are summarized in Table 2. Values range from 0 to about 1.5 m and are evidently correlated with

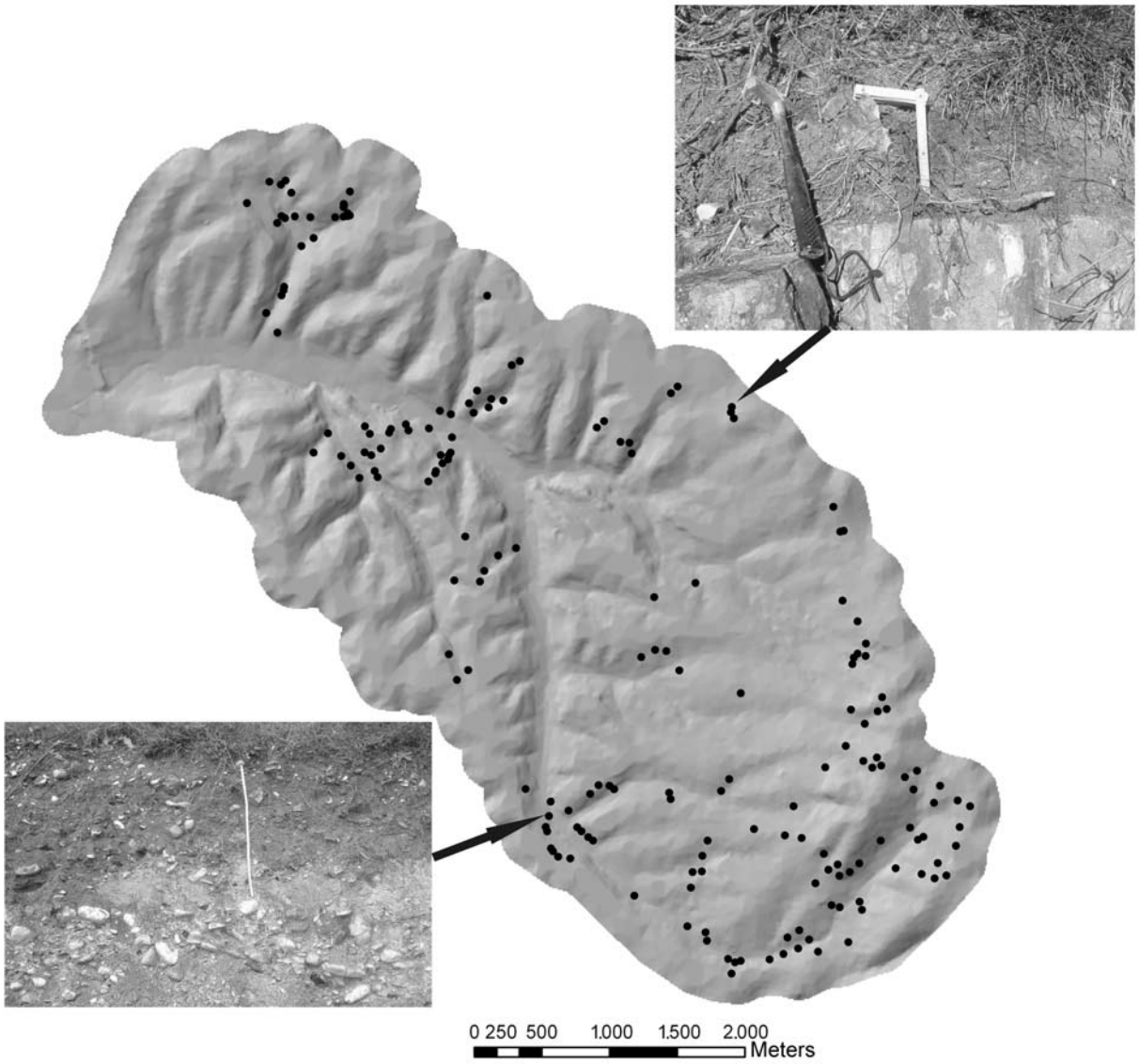

Figure 3. Location of the soil depth measurements in the Terzona basin.

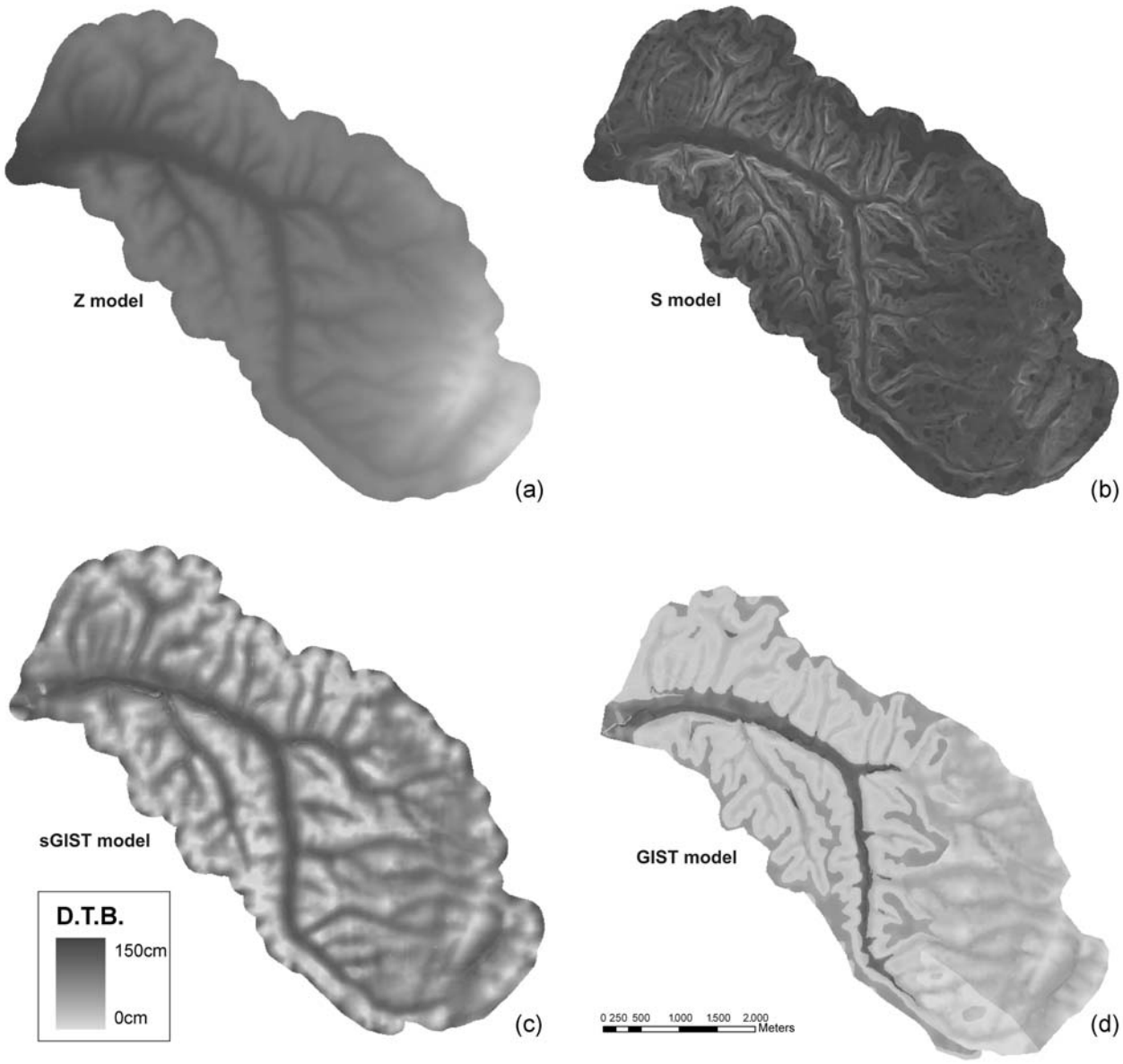

Figure 4. DTB maps produced by different soil depth models: (a) elevation-dependent (*Z*) model, (b) slope-gradient-dependent (*S*) model, (c) simplified GIST (sGIST) model, and (d) complete geology- and geomorphology-dependent (GIST) model.

lithology. Fifty five direct measurements were used to calibrate each class leading to the definition of a set of K_c values. The same subset of points was used also to define the p–η trend for each TLU. The remaining 162 surveyed points were used for model validation and for comparing the performance of different approaches.

[33] GIST was compared against two other approaches (proposed by *Saulnier et al.* [1997]) often used in large-scale regional analyses. These correlate soil depth to elevation and slope, respectively. The first (here called the *Z model*) expresses soil depth solely as a function of local elevation (z_i) and has the form

$$h_i = h_{\max} - \frac{z_i - z_{\min}}{z_{\max} - z_{\min}}(h_{\max} - h_{\min}), \tag{7}$$

while the second (*S model*) correlates soil depth to the local slope angle θ

$$h_i = h_{\max}\left[1 - \frac{\tan\theta_i - \tan\theta_{\min}}{\tan\theta_{\max} - \tan\theta_{\min}}\left(1 - \frac{h_{\min}}{h_{\max}}\right)\right]. \tag{8}$$

In these equations h_i is DTB computed at pixel i, $h_{\max}$ and $h_{\min}$ are the maximum and minimum values of DTB measured in the area, z_i and θ_i are the local values of elevation and slope, respectively, at pixel i, while $z_{\max}$ and $z_{\min}$ (or $\theta_{\max}$ and $\theta_{\min}$) are the maximum and minimum values of elevation (or slope) encountered in the test site.

[34] Although the two models rely heavily on geomorphological simplifications, they are often used to estimate a spatially distributed soil depth field when a rapid, easy

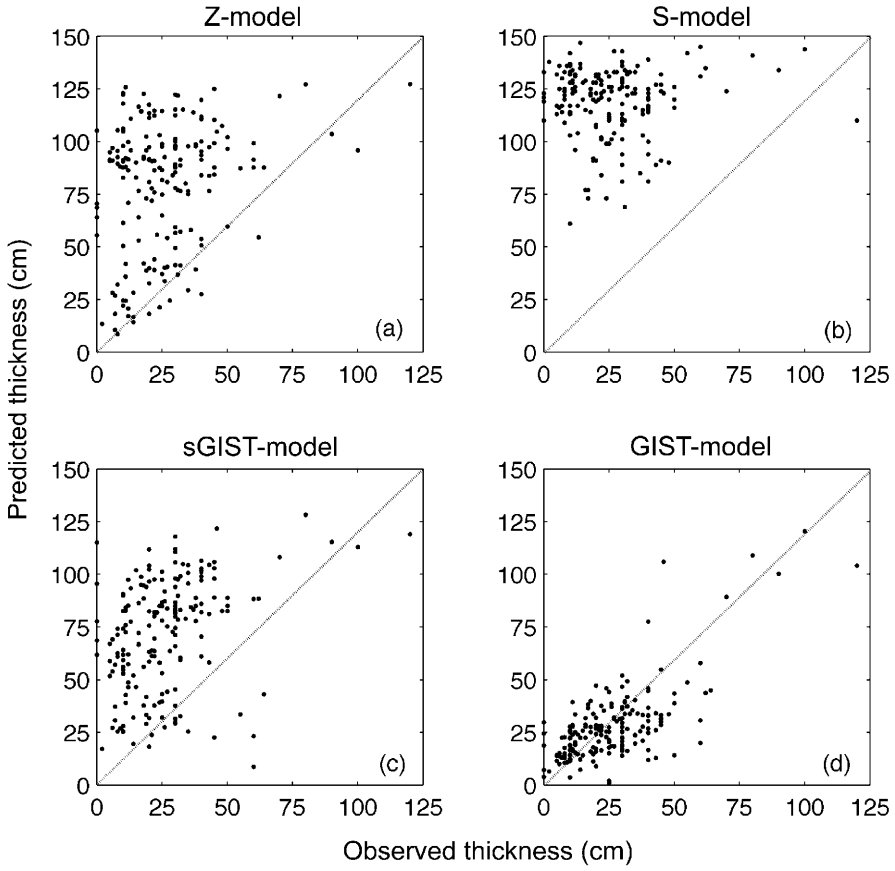

Figure 5. Model performance expressed as scatterplots of observed versus predicted values.

approach is needed in basin-scale modeling [e.g., *Salciarini et al.*, 2006]. All three models were applied to the Terzona Creek basin on a cell by cell basis (Figure 4). To further test the importance of geomorphology in GIST a simplified version of the model (*sGIST*), in which the TLUs are not differentiated on a geomorphological basis, was also applied (Figure 4c). The main differences between GIST and sGIST consist of the inverse correlation between curvature and DTB and in setting $\eta = p$ (soil depth assumed to invariantly increase downslope) in the latter. The results of all models were then compared to the 162 direct DTB measurements. A summary of the error statistics is presented in Table 3 and a visual comparison between predicted and observed data is shown in Figure 5.

[35] Errors in the estimation of h by the simple topographic models are substantial, both in terms of maximum and average absolute errors. The sGIST model produces slightly better results, with an average absolute error of about 47 cm. However, when geomorphology is taken into account (GIST model) the prediction improves markedly. Maximum absolute error (60 cm) and average absolute error (11 cm) are satisfactory for most applications requiring soil depth as an input variable.

5. Results and Model Comparisons

[36] The performance of the different models can be compared on the basis of error frequency distribution and the spatial structure of the error field. We propose that average DTB errors in applications regarding the predictive modeling of landslides and hydrological processes should not exceed 0.5 m. The impact of soil depth errors on spatial predictive models will be explored in detail in section 6.

[37] In the Z model the error distribution (Figure 6a) shows a bimodal trend with a first peak centered on acceptable values (average local error of about 15 cm) and a

Table 3. Comparison of Model Performance Against the Soil Depth Values Measured in the Field[a]

Model	Mean DTB (cm)	SD of DTB (cm)	Maximum Positive Error (cm)	Maximum Negative Error (cm)	Mean Absolute Error (cm)	SD of Absolute Error (cm)
Z	87.6	26.1	115	−12	54	29.92
S	126.4	15.5	140	−10	94	24.25
sGIST	64.6	30.9	115	−51	47	23.12
GIST	32.7	23.8	60	−40	11	8.54

[a]Here SD means standard deviation.

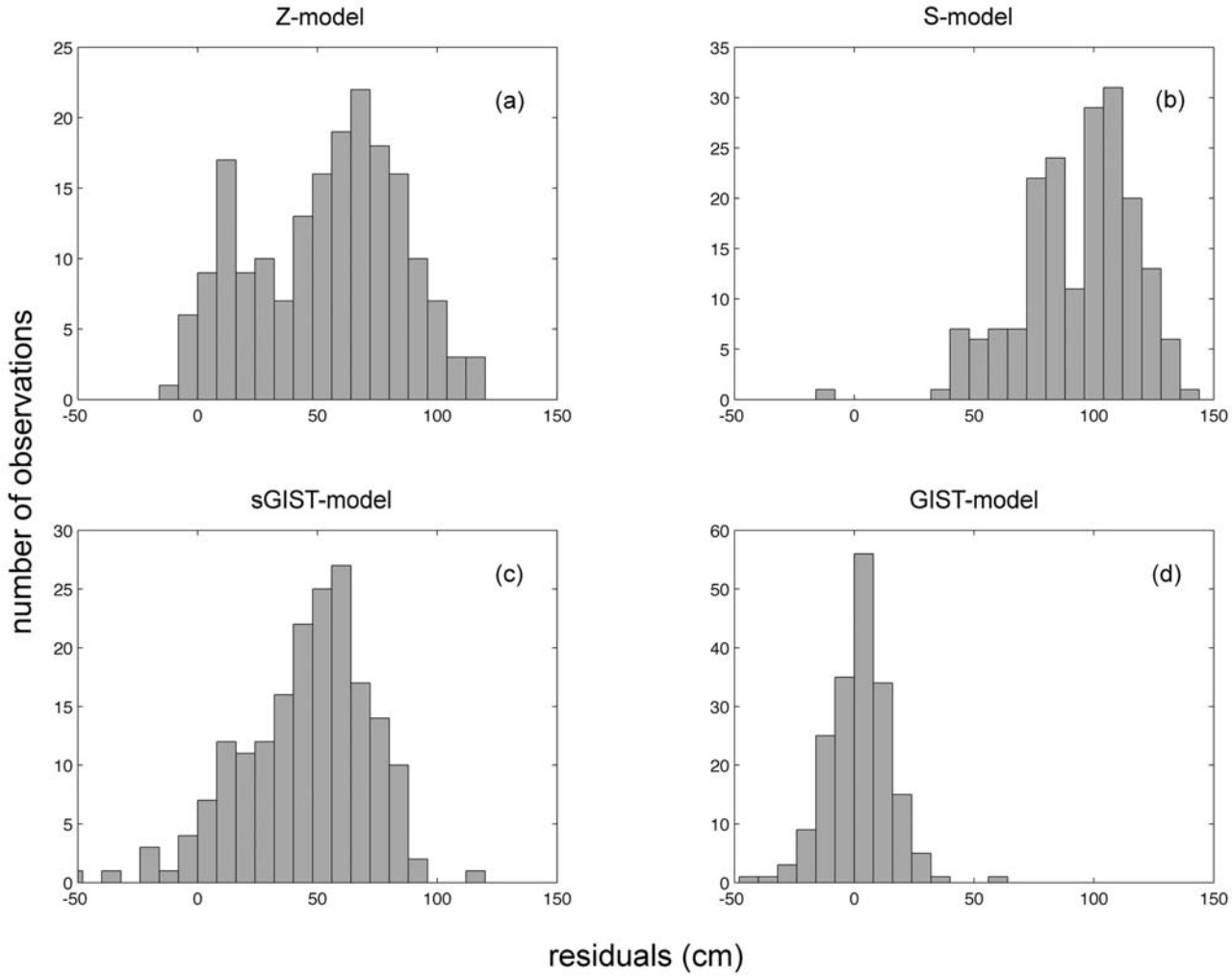

Figure 6. Frequency distribution of residuals for the four models. Residuals are expressed as the difference between predicted and observed soil thickness. Bin size is 8 cm.

second one, larger in frequency, centered on higher errors (~70 cm). This behavior points to two different types of errors, i.e., negative and positive deviations from the observed local values. Figure 7a shows the spatial distribution of errors for the *Z* model. Even though the pattern is to some extent controlled by the heterogeneous distribution of the validation points, the direct influence of elevation on the error structure remains evident. In valleys or at the footslopes soil depth is generally overestimated, while values on hilltops tend to be underestimated as a result of the lack of dependence of *h* on hillslope form, position and dominant processes. Only at the highest elevations in the southern portion of the basin are predicted and observed DTB values in agreement. However, in the Terzona basin this is mainly due to the fact that the higher elevations are incidentally occupied by scarcely weathered hard rock terrains, which have very low rates of soil production.

[38] The performance of the *S* model, which links DTB to slope gradient, is even less satisfactory. In the error frequency histogram (Figure 6b) a large single maximum is clearly centered on values of approximately 90 cm, indicating that soil depth is overestimated everywhere within the test area (Figure 7b). This is especially apparent in the upper portion of the basin where low gradient hilltops have thin regolith values. The few instances with relatively small prediction errors are related to granular soils in flat valleys, even though the model does not discriminate between the relatively wide alluvial plains in the lowest part of the basin and the narrower valleys at intermediate elevations, where DTB is low.

[39] The sGIST and GIST models have a more consistent behavior throughout the basin. The sGIST model performs slightly better than the *S* and *Z* models, with a mean absolute error of 47 cm and an error histogram that approximates a Gaussian distribution (Figure 6c). Small errors are quite homogeneously distributed throughout the basin and are especially concentrated near hilltops (in areas corresponding to the convex creep slope and to the seepage slope as per the classification of *Conacher and Dalrymple* [1977]) and on alluvial plains (Figure 7c).

[40] Most large errors occur at footslopes, especially in convex-concave-convex hillslopes in which the base of slope is only slightly convex. Underestimation of soil thickness takes place on the "Pianalto" top surface where the absence of geological information in the model does not allow the discrimination between rocky and soil-mantled hilltops.

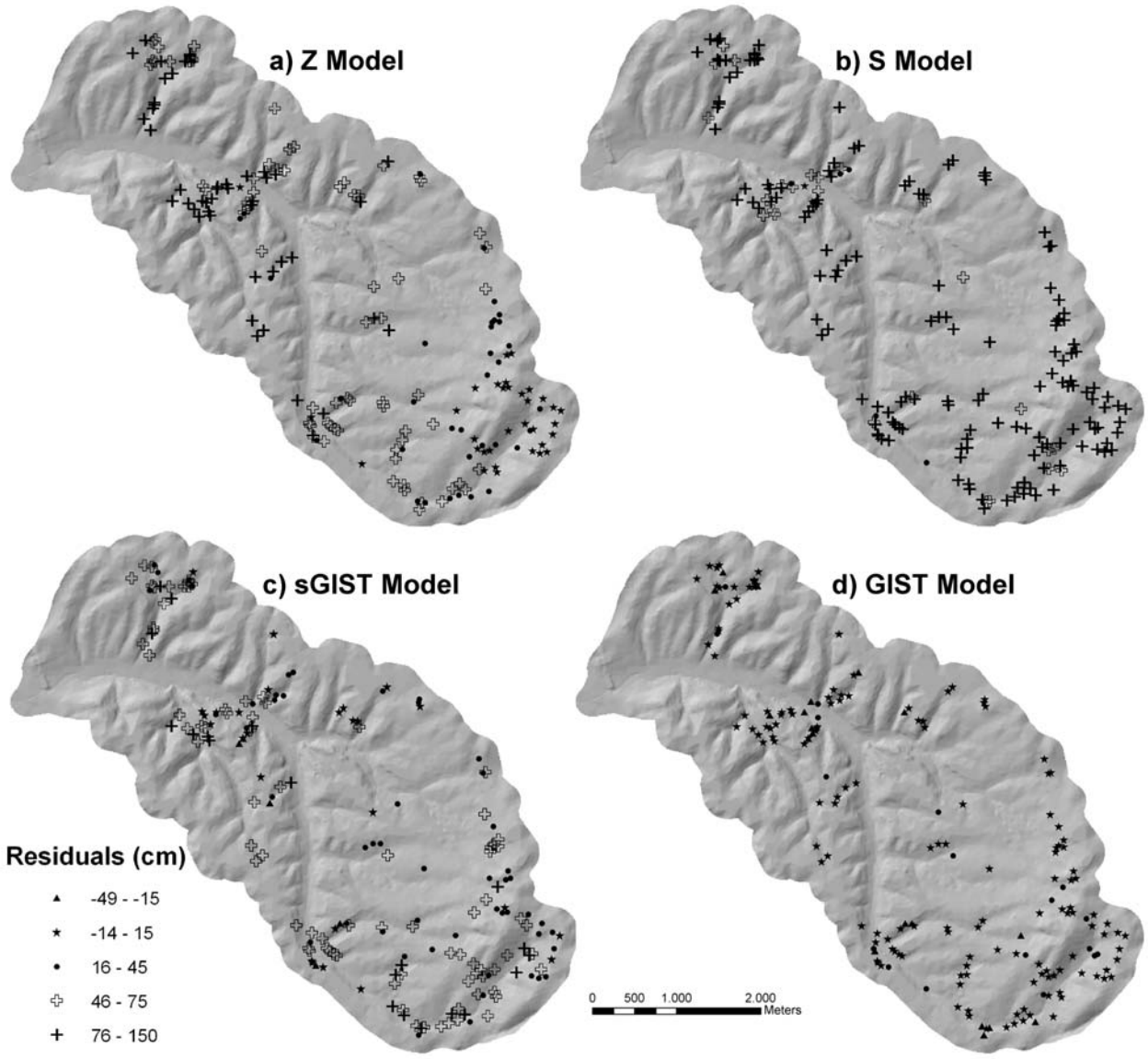

Figure 7. Spatial distribution of residuals (predicted minus observed values of soil thickness) for the four models. Note that black stars indicate errors of less than ±15 cm.

[41] These traits seem to be for the most part absent in the GIST model, in which differences in land-surface typology and geomorphology are taken into account explicitly. Model performance improves markedly as small errors (less than ±15 cm) are evenly distributed throughout the basin and the standard deviation is lower than in all other cases (Table 3 and Figure 6d). Underestimated DTB values, almost absent in all other models, are as common as the overestimated values. The histogram has a Gaussian distribution with a mean that is just above zero. The largest underestimated values usually occur over conglomerate outcrops in the upper medium part of hillslope profiles, although several correct DTB predictions are also present in the same areas.

[42] In general, the spatial distribution of residuals is homogeneous and the relatively few larger errors (greater than 15 cm) seem to be correlated to local causes (Figure 7d) that are not explicitly accounted for in the GIST model but that can influence soil balance along the hillslope profile, such as vegetation cover and agricultural practices.

6. Discussion and Hydrogeological Applications

[43] The advantage of having a basin-scale-distributed DTB map in geological and hydrological applications can be better understood by coupling the results with spatial or temporal predictive models for surface processes. Shallow landslides, one of the most common natural hazards in central Italy, are ideal for this purpose.

[44] The fundamental role of soil depth in controlling shallow landsliding has been known for some time. In particular, several authors have investigated the relative importance of the different parameters of slope stability [e.g., *Johnson and Sitar*, 1990; *Wu and Sidle*, 1995; *Van Asch et al.*, 1999; *Catani et al.*, 2005] and have attempted

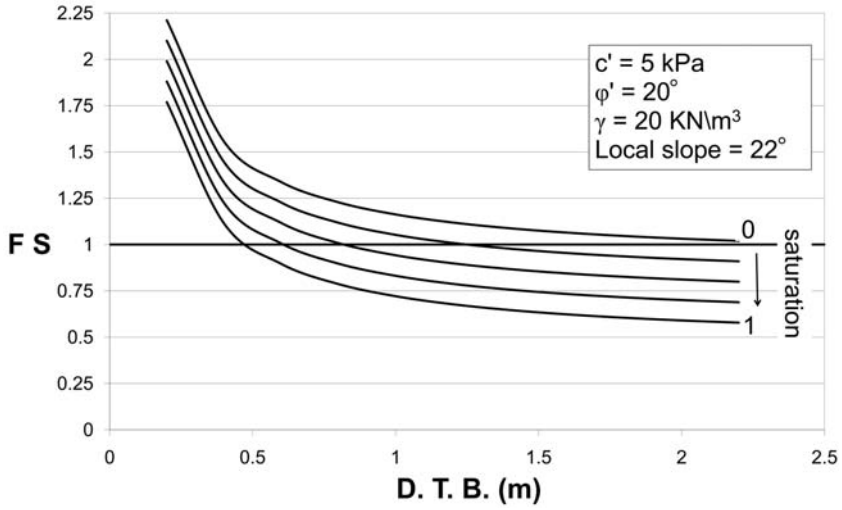

Figure 8. Graph of FS (calculated by means of the infinite slope formula of *Skempton and Delory* [1957]) versus soil depth for five different soil saturation values. Soil depth is perhaps the most significant parameter controlling the factor of safety.

to estimate the role played by soil depth in the overall stability of slopes. Figure 8 easily shows that soil depth is one of the most significant parameters controlling the factor of safety (FS). This is especially true for depths of less than 1.5 m, within which small variations produce very rapid changes in the FS (Figure 8).

[45] The large soil depth errors produced by the *Z*, *S*, and sGIST model can compromise the reliability of slope stability or rainfall-runoff applications. The reduction in DTB errors produced by the GIST model should lead to significant improvements in applications of this type.

[46] The relative control that soil depth has on process modeling was assessed by applying a distributed slope stability model to the Terzona basin. The slope stability model [*Leoni*, 2009; F. Catani et al., Real-time forecasting of landslides using meteorological radar and numerical modeling, submitted to *Landslides*, 2010] that was used derives from the classical infinite slope model of *Skempton and Delory* [1957] as modified by *Iverson* [2000], who added a "hydrologic term" that takes into account a spatially and time distributed pressure head. This model provides a spatial estimate of the FS and its evolution through time, and takes into account the apparent cohesion forces (produced by suction) in unsaturated soils

$$FS = \frac{\tan\varphi}{\tan\theta} + \frac{(c + c'(\psi))}{\gamma_s h \sin\theta\cos\theta} + \frac{\psi(h,t)\gamma_w \tan\varphi}{\gamma_s h \sin\theta\cos\theta}. \qquad (9)$$

Model input comprises morphometric data (soil thickness h and slope gradient θ) and geotechnical parameters (cohesion c, soil friction angle φ, soil unit weight γ_s, water unit weight γ_w). Pressure head ψ is computed making use of hydraulic conductivity measures and rainfall intensity through time. The FS is calculated pixel by pixel at different time steps; FS values less than one indicate an unstable slope. For further explanations on equation (9) see Catani et al. (submitted manuscript, 2010).

[47] As the objective of this part is to assess the utility of the GIST model for predicting landslide potential, the slope stability model was run four times using the different DTB patterns obtained from the four DTB models. Soil slips can develop at any depth between the topographic surface and the soil – bedrock interface. The maximum slip surface depth is equal to the predicted DTB value. All other parameters in the equation are held constant: any differences in the spatial distribution of FS depend only on the DTB patterns generated by the four soil depth models. Table 1 lists the geotechnical parameters used in the slope stability analysis of the lithologies in the Terzona basin (γ_s is held constant at 20 KNm^3). The values are consistent with other works carried out on sites in the area characterized by similar lithologies [*Bianchi et al.*, 2001; *Focardi and Garzonio*, 1983; *Canuti et al.*, 1982]. Hydraulic conductivity was measured in situ for every lithology (Table 1) using a constant head permeameter [*Amoozegar*, 1989]. The slope angle was obtained from the DTM. A rainfall event recorded in November 2008 by two raingauges a few kilometers from the Terzona basin was used. The event has a ten year return period and was characterized by a cumulative rainfall of 87 mm in 24 h with a peak intensity of 31 mm/h.

[48] Figure 9 illustrates the factor of safety produced by the slope stability model for the four soil thicknesses. The basin is partitioned into landslide hazard classes according to FS value: high (FS $\leq$ 1), moderate (1 > FS $\leq$ 1.3), and low (FS > 1.3).

[49] A recently updated landslide inventory in the area indicates that the rainfall event used in the simulation did not trigger any shallow landslide in the Terzona basin. Validation can therefore only be performed by quantifying the number of false positives (i.e., wrong predictions) produced by the slope stability model in the prediction of shallow slope failures in the basin. The assumption is that a correct soil depth will produce a smaller number of false positives. Table 4 lists the results of the slope stability modeling. The run that uses the GIST soil depth produces by far the best results as only 2% of the basin is classified within the highest-hazard class and 98% is in the class characterized as stable.

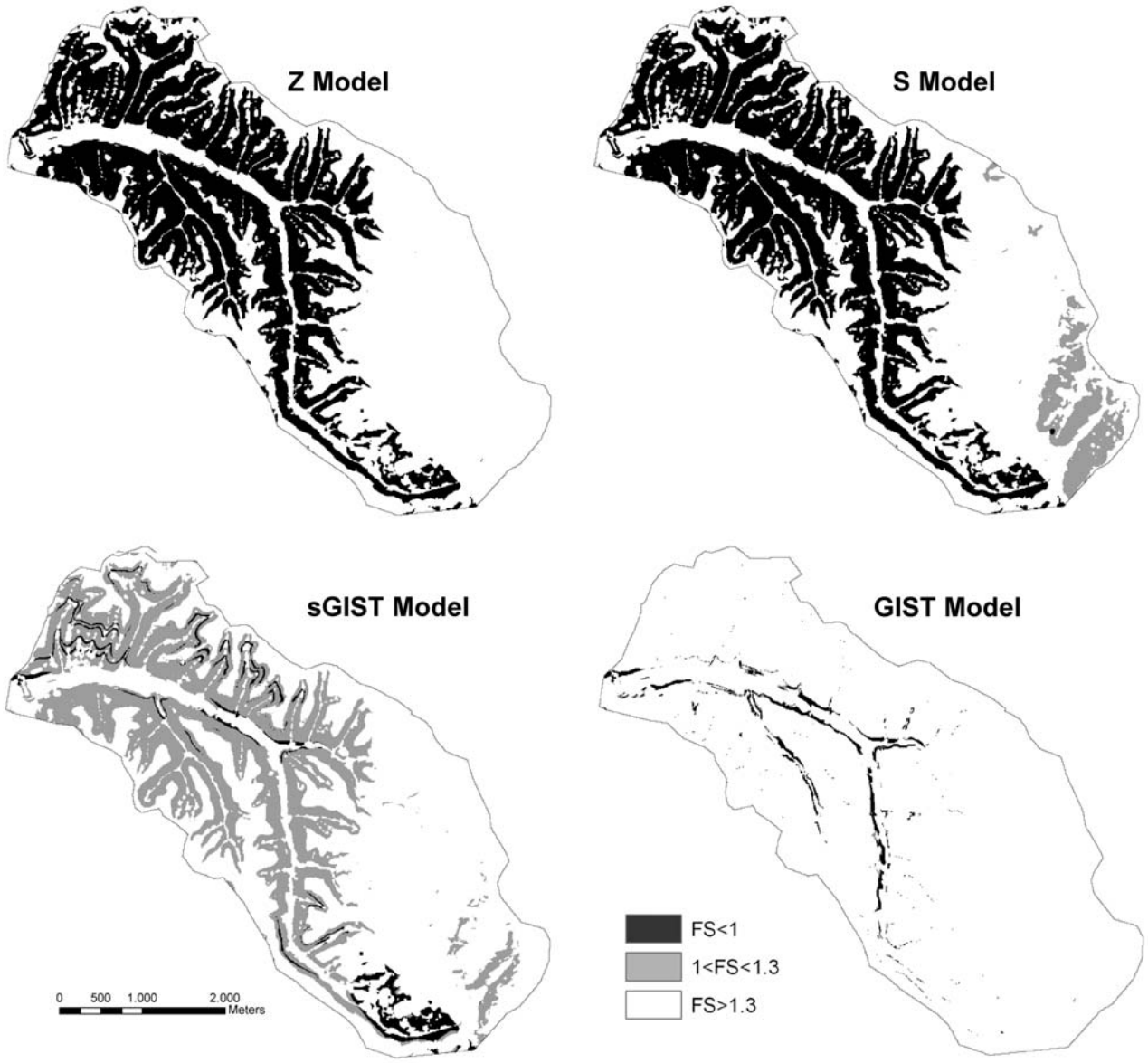

Figure 9. Factor of safety maps produced using the DTB values generated by the different soil depth models.

[50] The slope- (S) and elevation-based (Z) models, on the other hand, both place approx. 40% of the basin within the high-hazard class and only 55 and 60%, respectively, are classified as stable. Another simulation, performed considering a smaller rainfall event (44 mm in 3 hours following a dry spell), produced similar results, indicating that the use of soil depths from the S and Z models cause significant overestimation of the landslide hazard; even small amounts of precipitation are sufficient to destabilize the entire area of the basin occupied by shales or pliocenic terrains.

[51] The sGIST derived soil depth produces intermediate results, with 3.5% of the basin classified as high hazard and 64.5% ranked as stable. In this case, the spatial distribution of FS suggests two main considerations. First, the inclusion of three morphometric attributes produces a less unreliable FS distribution. For example, the stability of the pliocenic terrains increases significantly compared to the S and Z based slope stability computations, in good agreement with the local morphology. Conversely, the lack of geological input in sGIST is evident in the erroneous delineation of high-hazard areas in the shales (see Figure 1).

7. Conclusions

[52] GIST is a newly developed empirical model for the prediction of distributed soil thickness at basin scale. Soil

Table 4. Landslide Hazard Classification[a]

Model	Class 1 (High Hazard, FS ≤ 1)	Class 2 (Low Hazard, 1 < FS < 1,3)	Class 3 (Stable Areas, FS ≥ 1,3)
S	40.1%	4.8%	55.1%
Z	40.0%	0.1%	59.9%
sGIST	3.5%	32.1%	64.5%
GIST	1.9%	0.4%	97.7%

[a]Percentages express the portion of the basin within each hazard class.

depth patterns produced by the model provide significant benefits for other process based applications such as slope stability models. A key difference with other empirical models is the use of three morphometric attributes (curvature, position along the hillslope profile and slope gradient). The combined use of such attributes noticeably improves DTB estimation. However, the primary difference with traditional approaches is that geomorphology and lithology are also accounted for. This produces a further, significant improvement in model performance. The sGIST model, which lacks the geologically driven parameterization of the variables, generates larger DTB errors than the full GIST model. The errors in this version have a spatial distribution that is linked to both the local geomorphology (footslopes of convex-concave-convex slopes) and to stratigraphy (local errors linked to the "Pianalto" surface). The main limitation of the simplified version is, in fact, the failure to discriminate between areas in which the topographic indexes are similar but DTB varies for stratigraphic or geomorphological reasons.

[53] The comparative slope stability analysis carried out in the Terzona basin highlighted that DTB values strongly influence the spatial distribution of the Factor of Safety. A validation based on the detection of false positives demonstrates that by far the best results are obtained by coupling the GIST-derived DTB values with the infinite slope stability model to generate the FS map. Further understanding of the impact of the GIST model on the prediction of shallow landslides can be gained from its application in areas where a severe rainfall event triggered numerous shallow landslides [*Segoni et al.*, 2009; Catani et al., submitted manuscript, 2009].

[54] DTB maps produced by GIST could also prove valuable for generating spatially variable soil transmissivity values in hydrological models. This type of application appears especially promising for rainfall-runoff predictions in small to medium size, high-relief catchments, where subsurface flow is prominent and small-scale soil depth variability can strongly influence water transfer behavior.

[55] **Acknowledgments.** The authors gratefully acknowledge Scott Tyler and three anonymous referees for careful revision of the manuscript and their important contribution to the final quality of the paper through their comments and suggestions.

References

Amoozegar, A. (1989), Compact constant head permeameter for measuring saturated hydraulic conductivity of the vadose zone, *Soil Sci. Soc. Am. J.*, *53*, 1356–1361.

Armstrong, A. C. (1987), Slopes, boundary conditions and the development of convexo-concave forms—Some numerical experiments, *Earth Surf. Processes Landforms*, *12*, 17–30, doi:10.1002/esp.3290120104.

Arnett, R. R., and A. J. Conacher (1973), Drainage basin expansion and the nine unit landsurface model, *Aust. Geogr.*, *12*, 237–249.

Benvenuti, M., A. Bertini, C. Conti, and S. Dominici (2007), Integrated analyses of litho- and biofacies in a Pliocene cyclothemic, alluvial to shallow marine succession (Tuscany, Italy), *Geobios*, *40*, 143–158, doi:10.1016/j.geobios.2006.08.001.

Beven, K. J., and M. J. Kirkby (1979), A physically based variable contributing area model of basin hydrology, *Hydrol. Sci. Bull.*, *24*(1), 43–69.

Bianchi, F., F. Catani, and S. Moretti (2001), Environmental accounting of hillslopes processes in central Tuscany, Italy, in *Ecosystems and Sustainable Development III*, edited by Y. Villacampa, C. A. Brebbia, and J. L. Uso, pp. 229–238, WIT Press, Southampton, U. K.

Bierman, P., and E. J. Steig (1996), Estimating rates of denudation using cosmogenic isotope abundances in sediment, *Earth Surf. Processes Landforms*, *21*, 125–139, doi:10.1002/(SICI)1096-9837(199602)21:2<125::AID-ESP511>3.0.CO;2-8.

Boer, M., G. Del Barrio, and J. Puigdefabregas (1996), Mapping soil depth classes in dry Mediterranean areas using terrain attributes derived from a digital elevation model, *Geoderma*, *72*, 99–118, doi:10.1016/0016-7061(96)00024-9.

Braun, J., A. M. Heimsath, and J. Chappel (2001), Sediment transport mechanisms on soil-mantled hillslopes, *Geology*, *29*(8), 683–686, doi:10.1130/0091-7613(2001)029<0683:STMOSM>2.0.CO;2.

Brundsen, D., J. C. Doornkamp, P. G. Fookes, D. K. C. Jones, and L. M. H. Kelley (1975), Geomorphological mapping techniques in highway engineering, *J. Inst. Highway Eng.*, *22*, 35–41.

Canuti, P., P. Focardi, C. A. Garzonio, G. Rodolfi, P. Vannocci, L. Boccacci, F. Frascati, S. Moretti, and R. Salvi (1982), Stabilità dei versanti nell'area rappresentativa di Montespertoli (Firenze): Carta geologico-tecnica, morfometrica e dell'uso del suolo, map, Selca Press, Florence, Italy.

Carson, M. A., and M. J. Kirkby (1972), *Hillslope Form and Process*, 475 pp., Cambridge Univ. Press, Cambridge, U. K.

Catani, F., N. Casagli, L. Ermini, G. Righini, and G. Menduni (2005), Landslide hazard and risk mapping at catchment scale in the Arno River basin, *Landslides*, *2*, 329–342, doi:10.1007/s10346-005-0021-0.

Conacher, A. J., and J. B. Dalrymple (1977), The nine unit landsurface model: An approach to pedogeomorphic research, *Geoderma*, *18*, 1–153, doi:10.1016/0016-7061(77)90077-5.

Densmore, A. L., R. S. Anderson, B. G. McAdoo, and M. A. Ellis (1997), Hillslope evolution by bedrock landslides, *Science*, *275*, 369–372, doi:10.1126/science.275.5298.369.

Densmore, A. L., M. A. Ellis, and R. S. Anderson (1998), Landsliding and the evolution of normal-fault-bounded mountains, *J. Geophys. Res.*, *103*(B7), 15,203–15,219.

Dietrich, W. E., R. Reiss, M. L. Hsu, and D. R. Montgomery (1995), A process-based model for colluvial soil depth and shallow landsliding using digital elevation data, *Hydrol. Processes*, *9*, 383–400, doi:10.1002/hyp.3360090311.

Focardi, P., and C. A. Garzonio (1983), La frana di Marcialla (Certaldo, FI), *Geol. Tec.*, *1/83*, 13–19.

Gabet, E. J., and T. Dunne (2003), A stochastic sediment delivery model for a steep Mediterranean landscape, *Water Resour. Res.*, *39*(9), 1237, doi:10.1029/2003WR002341.

Gessler, P. E., I. D. Moore, N. J. McKenzie, and P. J. Ryan (1995), Soil-landscape modelling and spatial prediction of soil attributes, *Int. J. Geogr. Inf. Sci.*, *9*, 421–432, doi:10.1080/02693799508902047.

Gessler, P. E., O. A. Chadwick, F. Chamran, L. Althouse, and K. Holmes (2000), Modeling soil-landscape and ecosystem properties using terrain attributes, *Soil Sci. Soc. Am. J.*, *64*, 2046–2056.

Gilbert, G. K. (1877), Report on the geology of the Henry Mountains, in *U. S. Geographical and Geological Survey of the Rocky Mountain Region*, edited by J. W. Powell, 160 pp., Gov. Print. Off., Washington, D. C.

Goodman, A. (1999), Trend surface analysis in the comparison of spatial distributions of hillslope parameters, Ph.D. thesis, Deakin Univ., Geelong, Victoria, Australia. (Available at http://www.deakin.edu.au/agoodman/masters/.)

Hack, J. T. (1960), Interpretation of erosional topography in humid temperate regions, *Am. J. Sci.*, *258A*, 80–97.

Heimsath, A. M., W. E. Dietrich, K. Nishiizumi, and R. C. Finkel (1997), The soil production function and landscape equilibrium, *Nature*, *388*, 358–361, doi:10.1038/41056.

Heimsath, A. M., W. E. Dietrich, K. Nishiizumi, and R. C. Finkel (1999), Cosmogenic nuclides, topography, and the spatial variation of soil depth, *Geomorphology*, *27*, 151–172, doi:10.1016/S0169-555X(98)00095-6.

Heimsath, A. M., J. Chappell, W. E. Dietrich, K. Nishiizumi, and R. C. Finkel (2000), Soil production on a retreating escarpment in southeastern Australia, *Geology*, *28*, 787–790, doi:10.1130/0091-7613(2000)28<787:SPOARE>2.0.CO;2.

Heimsath, A. M., J. Chappel, W. E. Dietrich, K. Nishiizumi, and R. C. Finkel (2001a), Late Quaternary evolution in southeastern Australia: A field example using cosmogenic nuclides, *Quat. Int.*, *83–85*, 169–185, doi:10.1016/S1040-6182(01)00038-6.

Heimsath, A. M., W. E. Dietrich, K. Nishiizumi, and R. C. Finkel (2001b), Stochastic processes of soil production and transport: Erosion rates, topographic variation and cosmogenic nuclides in the Oregon coast range, *Earth Surf. Processes Landforms*, *26*, 531–552, doi:10.1002/esp.209.

Hillel, D. (1980), *Fundamentals of Soil Physics*, 413 pp., Academic, San Diego, Calif.

Hillel, D. (1998), *Environmental Soil Physics*, 771 pp., Academic, San Diego, Calif.

Iverson, R. M. (2000), Landslide triggering by rain infiltration, *Water Resour. Res.*, *36*, 1897–1910.

Jenny, H. (1941), *Factors of Soil Formation: A System of Quantitative Pedology*, McGraw-Hill, New York.

Jenny, H. (1980), *The Soil Resource*, 377 pp., Springer, Heidelberg, Germany.

Johnson, K. A., and N. Sitar (1990), Hydrologic conditions leading to debris–flow initiation, *Can. Geotech. J.*, *27*, 789–801, doi:10.1139/t90-092.

Leoni, L. (2009), Shallow landslides triggered by rainfall: Integration between ground-based weather radar and slope stability models in near-real-time, Ph.D. thesis, Univ. degli Stud. di Firenze, Florence, Italy.

Lexer, M. J., and K. Honninger (1998), Estimating physical soil parameters for sample plots of large-scale forest inventories, *For. Ecol. Manage.*, *111*, 231–247, doi:10.1016/S0378-1127(98)00335-1.

Liang, S. (1997), An investigation of remotely–sensed soil depth in the optical region, *Int. J. Remote Sens.*, *18*(16), 3395–3408, doi:10.1080/014311697216946.

Martin, Y. (2000), Modelling hillslope evolution: Linear and nonlinear transport relations, *Geomorphology*, *34*, 1–21, doi:10.1016/S0169-555X(99)00127-0.

Martini, I. P., and G. B. Vai (2001), *Anatomy of an Orogen: The Apennines and Adjacent Mediterranean Basins*, 632 pp., Kluwer Acad., Dordrecht, Netherlands.

McFadden, L. D., and P. L. K. Knuepfer (1990), Soil geomorphology: The linkage of pedology and surficial processes, *Geomorphology*, *3*, 197–205, doi:10.1016/0169-555X(90)90003-9.

Milne, G. (1935), Some suggested units for classification and mapping, particularly for east African soils, *Soil Res.*, *4*, 183–198.

Minasny, B., and A. B. McBratney (1999), A rudimentary mechanistic model for soil production and landscape development, *Geoderma*, *90*, 3–21, doi:10.1016/S0016-7061(98)00115-3.

Minasny, B., and A. B. McBratney (2001), A rudimentary mechanistic model for soil production and landscape development: Part II. A two-dimensional model incorporating chemical weathering, *Geoderma*, *103*, 161–179, doi:10.1016/S0016-7061(01)00075-1.

Montgomery, D. R., and M. T. Brandon (2002), Topographic controls on erosion rates in tectonically active mountain ranges, *Earth Planet. Sci. Lett.*, *201*, 481–489, doi:10.1016/S0012-821X(02)00725-2.

Moore, I. D., and G. J. Burch (1986), Sediment transport capacity of sheet and rill flow: Application of unit stream power theory, *Water Resour. Res.*, *22*, 1350–1360, doi:10.1029/WR022i008p01350.

Moore, I. D., P. E. Gessler, and G. A. Nielson (1993), Soil attribute prediction using terrain analysis, *Soil Sci. Soc. Am. J.*, *57*, 443–452.

Mudd, S. M., and D. J. Furbish (2004), Influence of chemical denudation on hillslope morphology, *J. Geophys. Res.*, *109*, F02001, doi:10.1029/2003JF000087.

Mudd, S. M., and D. J. Furbish (2006), Using chemical tracers in hillslope soils to estimate the importance of chemical denudation under conditions of downslope sediment transport, *J. Geophys. Res.*, *111*, F02021, doi:10.1029/2005JF000343.

Odeha, I. O. A., A. B. McBratney, and D. J. Chittleborough (1994), Spatial prediction of soil properties from a digital elevation model, *Geoderma*, *63*, 197–214, doi:10.1016/0016-7061(94)90063-9.

Park, S. J., K. McSweeney, and B. Lowery (2001), Identification of the spatial distribution of soils using a process-based terrain characterization, *Geoderma*, *103*, 249–272, doi:10.1016/S0016-7061(01)00042-8.

Rapisarda, F. (2007), Landslide analysis in Apennine chain areas, *Landslides*, *4*, 75–83, doi:10.1007/s10346-006-0066-8.

Reid, L. M., and T. Dunne (1996), *Rapid Evaluation of Sediment Budgets*, 164 pp., Catena, Reiskirchen, Germany.

Roering, J. J., J. W. Kirchner, and W. E. Dietrich (1999), Evidence for nonlinear, diffusive sediment transport on hillslopes and implications for landscape modeling, *Water Resour. Res.*, *35*, 853–870, doi:10.1029/1998WR900090.

Roering, J. J., J. W. Kirchner, L. S. Sklar, and W. E. Dietrich (2001), Hillsope evolution by nonlinear creep and landsliding: An experimental study, *Geology*, *29*(2), 143–146, doi:10.1130/0091-7613(2001)029<0143:HEBNCA>2.0.CO;2.

Saco, P. M., G. R. Willgoose, and G. R. Hancock (2006), Spatial organization of soil depths using a landform evolution model, *J. Geophys. Res.*, *111*, F02016, doi:10.1029/2005JF000351.

Salciarini, D., J. W. Godt, W. Z. Savage, P. Conversini, R. L. Baum, and J. A. Michael (2006), Modeling regional initiation of rainfall-induced shallow landslides in the eastern Umbria Region of central Italy, *Landslides*, *3*, 181–194, doi:10.1007/s10346-006-0037-0.

Saulnier, G. M., K. Beven, and C. Obled (1997), Including spatially variable effective soil depths in TOPMODEL, *J. Hydrol.*, *202*, 158–172, doi:10.1016/S0022-1694(97)00059-0.

Schlunegger, F., K. Detzner, and D. Olsson (2002), The evolution towards steady state erosion in a soil-mantled drainage basin: Semi-quantitative data from a transient landscape in the Swiss Alps, *Geomorphology*, *43*, 55–76, doi:10.1016/S0169-555X(01)00120-9.

Schumacher, T. E., M. J. Lindstrom, J. A. Schumacher, and G. D. Lemme (1999), Modeling spatial variation in productivity due to tillage and water erosion, *Soil Tillage Res.*, *51*, 331–339, doi:10.1016/S0167-1987(99)00046-X.

Segoni, S. (2008), Elaborazione ed applicazioni di un modello per la previsione dello spessore delle coperture superficiali, Ph.D. thesis, Univ. degli Stud. di Firenze, Florence, Italy.

Segoni, S., L. Leoni, A. I. Benedetti, F. Catani, G. Righini, G. Falorni, S. Gabellani, R. Rudari, F. Silvestro, and N. Rebora (2009), Towards a definition of a real-time forecasting network for rainfall induced shallow landslides, *Nat. Hazards Earth Syst. Sci.*, *9*, 2119–2133.

Selby, M. J. (1993), *Hillslope Materials and Processes*, 451 pp., Oxford Univ. Press, Oxford, U. K.

Skempton, A. W., and I. A. Delory (1957), Stability of natural slopes in London clay, paper presented at 4th International Conference on Soil Mechanics and Foundation Engineering, London, 12–24 Aug.

Tsai, C. C., Z. S. Chen, C. T. Duh, and F. V. Horng (2001), Prediction of soil depth using a soil-landscape regression model: A case study on forest soils in southern Taiwan, *Proc. Natl. Sci. Counc. Repub. China*, *25*(1), 34–49.

Tucker, G. E., F. Catani, A. Rinaldo, and R. L. Bras (2001), Statistical analysis of drainage density from digital terrain data, *Geomorphology*, *36*(3–4), 187–202, doi:10.1016/S0169-555X(00)00056-8.

United States Soil Conservation Service (1975), *Soil Taxonomy: A Basic System of Soil Classification for Making and Interpreting Soil Surveys*, Gov. Print. Off., Washington, D. C.

Van Asch, T. W. J., J. Buma, and L. P. H. Van Beek (1999), A view on some hydrological triggering systems in landslides, *Geomorphology*, *30*(1–2), 25–32, doi:10.1016/S0169-555X(99)00042-2.

Wu, W., and R. C. Sidle (1995), A distributed slope stability model for steep forested basins, *Water Resour. Res.*, *31*(8), 2097–2110, doi:10.1029/95WR01136.

Ziadat, M. F. (2005), Analyzing digital terrain attributes to predict soil attributes for a relatively large area, *Soil Sci. Soc. Am. J.*, *69*, 1590–1599, doi:10.2136/sssaj2003.0264.

F. Catani, G. Falorni, and S. Segoni, Department of Earth Sciences, University of Firenze, Via La Pira 4, I-50121 Florence, Italy. (filippo.catani@unifi.it)